



Article

Functionalized KIT-6/Polysulfone Mixed Matrix Membranes for Enhanced CO₂/CH₄ Gas Separation

Thiam Leng Chew ^{1,2,*} , Sie Hao Ding ^{1,2}, Pei Ching Oh ^{1,2}, Abdul Latif Ahmad ³  and Chii-Dong Ho ⁴

¹ Department of Chemical Engineering, Universiti Teknologi PETRONAS, Seri Iskandar 32610, Perak, Malaysia; ding.sie_g03642@utp.edu.my (S.H.D.); peiching.oh@utp.edu.my (P.C.O.)

² CO₂ Research Centre (COSRES), Institute of Contaminant Management, Universiti Teknologi PETRONAS, Seri Iskandar 32610, Perak, Malaysia

³ School of Chemical Engineering, Engineering Campus, Universiti Sains Malaysia, Nibong Tebal 14300, Pulau Pinang, Malaysia; chlatif@usm.my

⁴ Department of Chemical and Materials Engineering, Tamkang University, New Taipei City 25137, Taiwan; cdho@mail.tku.edu.tw

* Correspondence: thiamleng.chew@utp.edu.my; Tel.: +605-3687626

Received: 30 July 2020; Accepted: 9 September 2020; Published: 9 October 2020



Abstract: The development of mixed matrix membranes (MMMs) for effective gas separation has been gaining popularity in recent years. The current study aimed at the fabrication of MMMs incorporated with various loadings (0–4 wt%) of functionalized KIT-6 (NH₂KIT-6) [KIT: Korea Advanced Institute of Science and Technology] for enhanced gas permeation and separation performance. NH₂KIT-6 was characterized by field emission scanning electron microscope (FESEM), X-ray diffraction (XRD), Fourier transform infrared (FTIR), and N₂ adsorption–desorption analysis. The fabricated membranes were subjected to FESEM and FTIR analyses. The effect of NH₂KIT-6 loading on the CO₂ permeability and ideal CO₂/CH₄ selectivity of the fabricated membranes were investigated in gas permeation and separation studies. The successfulness of (3-Aminopropyl) triethoxysilane (APTES) functionalization on KIT-6 was confirmed by FTIR analysis. As observed from FESEM images, MMMs with no voids in the matrix were successfully fabricated at a low NH₂KIT-6 loading of 0 to 2 wt%. The CO₂ permeability and ideal CO₂/CH₄ selectivity increased when NH₂KIT-6 loading was increased from 0 to 2 wt%. However, a further increase in NH₂KIT-6 loading beyond 2 wt% led to a drop in ideal CO₂/CH₄ selectivity. In the current study, a significant increase of about 47% in ideal CO₂/CH₄ selectivity was achieved by incorporating optimum 2 wt% NH₂KIT-6 into the MMMs.

Keywords: KIT-6; functionalization; mixed matrix membranes; CO₂; CH₄

1. Introduction

Polymer membranes have emerged as a potential candidate in carbon dioxide removal due to their economical alternatives to conventional separation processes. Membrane technology exhibits operational flexibility, small design, cost efficiency, easy scale-up, high product quality, and a small footprint [1–3]. However, polymer membranes commonly suffer from a trade-off between permeability and selectivity [4–10].

In view of the drawbacks of polymer membranes, which limit the application of polymer membranes in gas separation, development of mixed matrix membranes (MMMs) for gas separation applications has been gaining popularity among researchers in recent years. MMMs are commonly formed by incorporating inorganic fillers into the polymer matrix. Among the various inorganic fillers,

mesoporous silicas appear to be a highly potential filler in the MMMs for efficient gas permeation and separation [11]. Mesoporous silicas possess several advantages including high specific surface area, high mechanical and thermal stability, and high CO₂ adsorption capacity [12]. In addition, the high porosity of mesoporous silica facilitates gas permeation during gas separation [13].

KIT-6 (KIT: Korea Advanced Institute of Science and Technology) is a type of mesoporous silica, which is a highly potential filler for MMMs due to its large pore size. KIT-6 has drawn the attention of researchers for gas permeation and separation. Owing to the large pore size, KIT-6 is granted with an interpenetrating pore system, which enables the formation of an intimate structure with polymer matrix [4]. Intimate structure in MMMs is essential for high gas permeation and separation performance of MMMs.

The functionalization of mesoporous silica by amine groups is one of the methods to further enhance the gas permeation and separation performance of MMMs [14]. Wu et al. [14] found that by using polyethylenimine-functionalized-MCM-41 [MCM: Mobil Composition of Matter], better interfacial interaction could be formed with the polymer compared to unfunctionalized MCM-41. The amine-functionalized-MCM-41 resulted in improvement in CO₂ permeability and CO₂/CH₄ selectivity as compared to the MMMs incorporated with unfunctionalized MCM-41 [14]. Meanwhile, Kim and Marand [11] performed amine functionalization on MCM-41 filler, which resulted in great compatibility with glassy polysulfone (PSF) membrane and significantly enhanced CO₂/CH₄ selectivity of the MMMs [11]. Furthermore, Waheed et al. [1] reported that good dispersion and adhesion of the filler with the PSF polymer were achieved by functionalizing the rice husk silica (RHS) filler with 4-aminophenazone. The MMMs incorporated with amine-functionalized RHS displayed significantly higher CO₂/CH₄ selectivity as well as CO₂/N₂ selectivity [1]. On the other hand, Khan et al. [13] reported similar results where MCM-41 was functionalized with aminopropyltrimethoxysilane. The use of amine-functionalized-MCM-41 as a filler resulted in the elimination of voids as well as good dispersion of the filler in the MMMs along with significantly higher CO₂/CH₄ and CO₂/N₂ selectivities [13]. Thus, amine functionalization on the mesoporous silica filler would significantly improve the structure of the MMMs by reducing or eliminating the void formations in MMMs, which will then enhance the gas permeation and separation performance of the MMMs.

The aim of this study was to investigate the effect of incorporation of amine-functionalized-KIT-6 filler on the CO₂ and CH₄ gas permeability and selectivity performance of the MMMs. The KIT-6 was functionalized with (3-Aminopropyl) triethoxysilane (APTES). The functionalized KIT-6 was incorporated into the PSF polymer matrix to fabricate different MMMs. PSF is a type of polymer with good thermomechanical stability, gas permeability, and selectivity [15–19]. The functionalized KIT-6 and the fabricated MMMs were characterized using different analytical techniques. The fabricated MMMs were subjected to CO₂ and CH₄ gas permeation and separation at 25 °C.

2. Materials and Methods

2.1. Chemicals and Materials Used

(3-Aminopropyl) triethoxysilane (APTES, 99.8%) and polysulfone (PSF) were purchased from Sigma Aldrich. Tetrahydrofuran (THF, 99.8%) was purchased from Merck. All chemicals were used without purification.

2.2. Functionalization of KIT-6

KIT-6 (1 g) was dispersed in 100 milliliters of dry toluene in a flask. To this solution, 9.0 mmol of APTES was added, and the functionalization of KIT-6 was carried out by refluxing the resulting solution at 80 °C for 24 h [20]. The functionalized KIT-6 sample was filtered, washed with 50:50 distilled water and ethanol mixture, followed by acetone. The obtained sample was dried overnight at room temperature, followed by drying in a vacuum oven at 80 °C for 16 h. The functionalized samples were named as NH₂KIT-6.

2.3. Preparation of the Membranes

Preparation of NH₂KIT-6/PSF MMMs (which were incorporated with functionalized KIT-6) were conducted following previously reported procedures with some modifications [11,21]. A desired loading (0–4 wt%) of NH₂KIT-6 was added to 10 mL of THF, followed by ultrasonication for 30 min. The PSF pellet was added and dissolved into the solution for 18 h. Then, the solution was sonicated for 30 min to remove air bubbles, and subsequently was cast on a glass plate using a casting blade with a gap of 200 μm. The glass plate was covered and left for 3 days at room temperature to ensure complete solvent evaporation. The prepared membranes were peeled off and stored in desiccators.

2.4. Characterizations of KIT-6, NH₂KIT-6, and the Membranes

The morphology of the NH₂KIT-6 filler was analyzed by FESEM (VPFESEM, Zeiss Supra55 VP). NH₂KIT-6 were subjected to XRD (X'Pert³ Powder & Empyrean, PANalytical) scanning for crystalline structure study. Functional groups in KIT-6 and NH₂KIT-6 were determined by FTIR (Perkin Almer, Frontier). The pore characteristics of KIT-6 and NH₂KIT-6 were analyzed using N₂ adsorption–desorption analysis (TriStar II 3020 V1.04) with liquid nitrogen at 77 K. The specific surface area of the sample was calculated by using the Brunauer–Emmett–Teller (BET) method. The mesopore size distribution was determined by using the Barrett–Joyner–Halenda (BJH) method. The morphology of the fabricated membranes was analyzed by FESEM (VPFESEM, Zeiss Supra55 VP). The membranes were also subjected to FTIR analysis (Perkin Almer, Frontier).

2.5. Gas Permeation and Separation Studies

The membrane was sealed in a membrane gas cell that was connected to the membrane gas permeation and separation test system. CO₂ or CH₄ gas with a purity of 99.99% was fed separately to the membrane gas permeation and separation system. The gas permeation was performed at 25 °C. The pressure difference was regulated to be 5 bar or 7 bar. The permeate flow was measured using a bubble flow meter. The gas permeability, P , was calculated using Equation (1):

$$P = \frac{Nl}{(P_f - P_p)A} \quad (1)$$

where l is the membrane thickness, N is the permeate flow, P_f is the feed pressure, P_p is the permeate pressure, and A is the membrane area.

The ideal selectivity, α of the membrane was calculated as the ratio of CO₂ gas permeance to CH₄ gas permeance.

Each gas permeation measurement was repeated three times.

3. Results and Discussion

3.1. Characterizations of NH₂KIT-6

Figure 1 shows the FESEM image of NH₂KIT-6. The FESEM image of NH₂KIT-6 revealed the typical rock-like morphology. Figure 2 shows the XRD pattern of NH₂KIT-6, which exhibits peak diffractions of about 1.1° at 2θ. This shows that the samples had the ordered mesostructure with a three-dimensional cubic Ia3d symmetry [22]. The XRD pattern of the NH₂KIT-6 sample in the current project is in agreement with the XRD pattern for KIT-6 reported by Ayad et al. [22].

The FTIR spectra of KIT-6 and NH₂KIT-6 are shown in Figure 3. The characteristic band at 3464 cm⁻¹ indicates the stretching vibration of hydrogen bonding from silanol group $\gamma(\equiv\text{Si}-\text{OH})$ [23]. Furthermore, the characteristic band at 1640 cm⁻¹ indicates the O–H bending vibration mode. The anti-symmetric and symmetric stretching vibrations of Si–O–Si groups are observed at characteristic bands at 1083 cm⁻¹ and 804 cm⁻¹, respectively [24]. It is interesting to observe the characteristic band at 1459 cm⁻¹, which is present in the FTIR spectra of NH₂KIT-6 but is absent in the FTIR spectra of KIT-6. This characteristic

band at 1459 cm^{-1} indicates the appearance of N–H bonds in $\text{NH}_2\text{KIT-6}$ and hence prove the successful amine-functionalization of KIT-6 [20,23,25]. In addition, the characteristic band at around 2926 cm^{-1} , which indicates the C–H stretching vibration of the organosilane, is observed in the FTIR spectra of $\text{NH}_2\text{KIT-6}$ but is not found in the spectra of KIT-6 [23]. This further proves the effective functionalization of KIT-6.

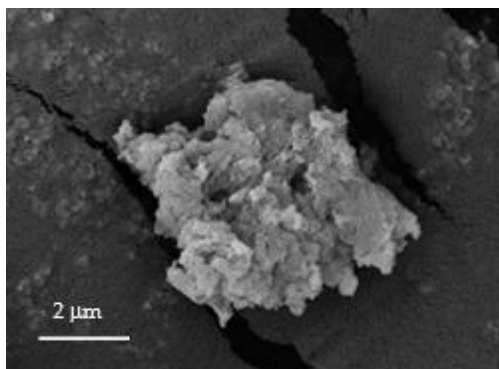


Figure 1. FESEM image of $\text{NH}_2\text{KIT-6}$.

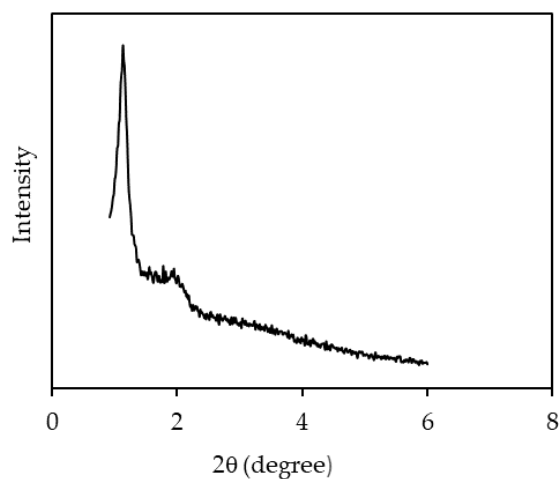


Figure 2. XRD pattern of $\text{NH}_2\text{KIT-6}$.

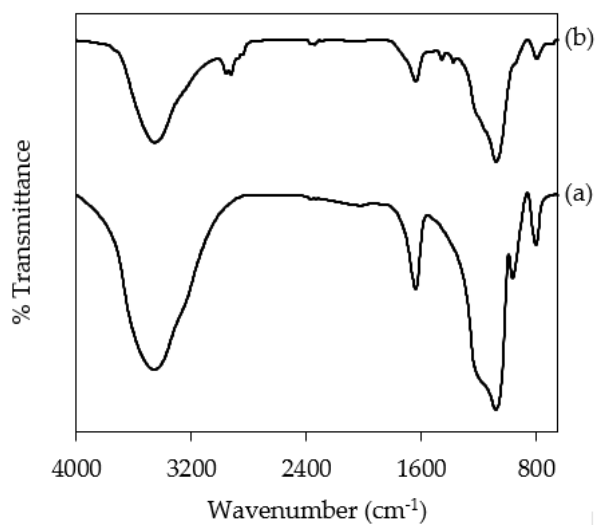


Figure 3. FTIR spectra of (a) KIT-6 and (b) $\text{NH}_2\text{KIT-6}$.

Figure 4 shows the nitrogen adsorption–desorption isotherms of KIT-6 and NH₂KIT-6. Type IV with a hysteresis loop from the nitrogen adsorption isotherms for KIT-6 and NH₂KIT-6 is observed, which represents the characteristic of a mesoporous material [4,5,20,26]. According to the IUPAC classification, a type H1 hysteresis loop can be observed from the isotherm; this indicates the characteristic of mesoporous materials and characteristic of material with interconnected large cylindrical pore geometry and a high degree of pore size uniformity [26]. In the current study, NH₂KIT-6 sample possessed a specific surface area of 108 m²/g, a pore volume of 0.18 cm³/g, and a pore diameter of 6.50 nm.

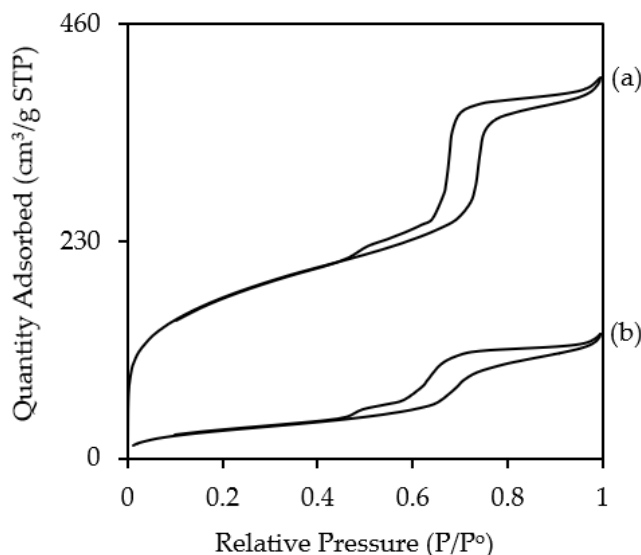


Figure 4. Nitrogen adsorption–desorption isotherm of (a) KIT-6 and (b) NH₂KIT-6.

3.2. Characterizations of the Membranes

Figure 5 shows the top view of FESEM images of NH₂KIT-6/PSF MMMs with different loadings of NH₂KIT-6. The particles observed indicate that NH₂KIT-6 was successfully incorporated into the PSF matrix [26]. Figure 6 shows the cross-sectional FESEM images of the NH₂KIT-6/PSF MMMs. Incorporating up to 2 wt% NH₂KIT-6 into the MMMs produced MMMs with no void in the matrix. After the functionalization of KIT-6 silica with APTES, the silane backbone of APTES promoted good silica–polymer interactions via van der Waals forces in the MMMs [25,27,28]. However, filler agglomeration was observed when NH₂KIT-6 loading in the MMMs was 4 wt%, as highlighted in Figure 6d.

The FTIR spectra of pristine PSF membrane and NH₂KIT-6/PSF MMMs are shown in Figure 7. As observed from Figure 7a, the pristine PSF membrane shows C–H rocking at the characteristic band at 831 cm^{−1}. The C–C stretching is indicated by characteristic bands at 1012 cm^{−1} and 1103 cm^{−1}. The Ar–SO₂–Ar symmetric stretching is observed at a characteristic band at 1147 cm^{−1}, where Ar corresponds to aromatic. On the other hand, the Ar–O–Ar stretching is observed at 1235 cm^{−1} and S=O symmetric stretching is observed at 1294 cm^{−1} [29]. Besides, the characteristic band at 2926 cm^{−1} indicates the C–H stretching vibration [1]. It is interesting to find about the interaction between NH₂KIT-6 filler and the PSF polymer phase where the characteristic bands of the PSF were retained in the FTIR spectra of the MMMs. This is in agreement with the FTIR analysis reported by Khary and Abdelsalam [30]. As observed from Figure 7b–e, a small characteristic band at 3464 cm^{−1}, which is assigned to the Si–OH group, was observed for the FTIR spectra of four NH₂KIT-6/PSF MMMs [23]. This indicates the presence of NH₂KIT-6 in the MMMs. The small characteristic band at 3464 cm^{−1}, which is due to the Si–OH group of the NH₂KIT-6, was not observed in the FTIR spectra of the pristine PSF membrane.

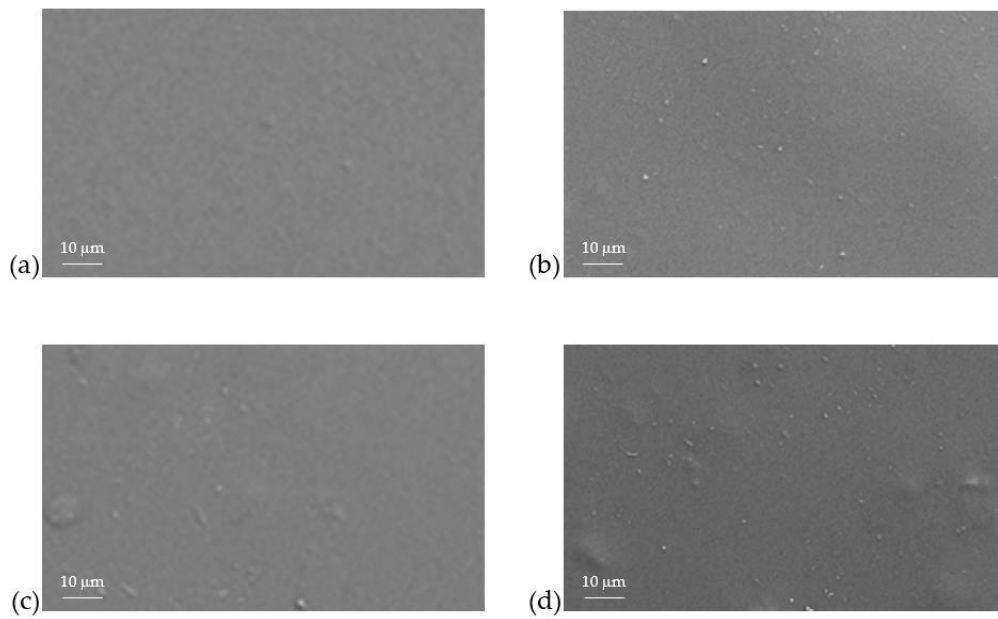


Figure 5. The top view of FESEM images of (a) 1% NH₂KIT-6/PSF, (b) 2% NH₂KIT-6/PSF, (c) 3% NH₂KIT-6/PSF, and (d) 4% NH₂KIT-6/PSF.

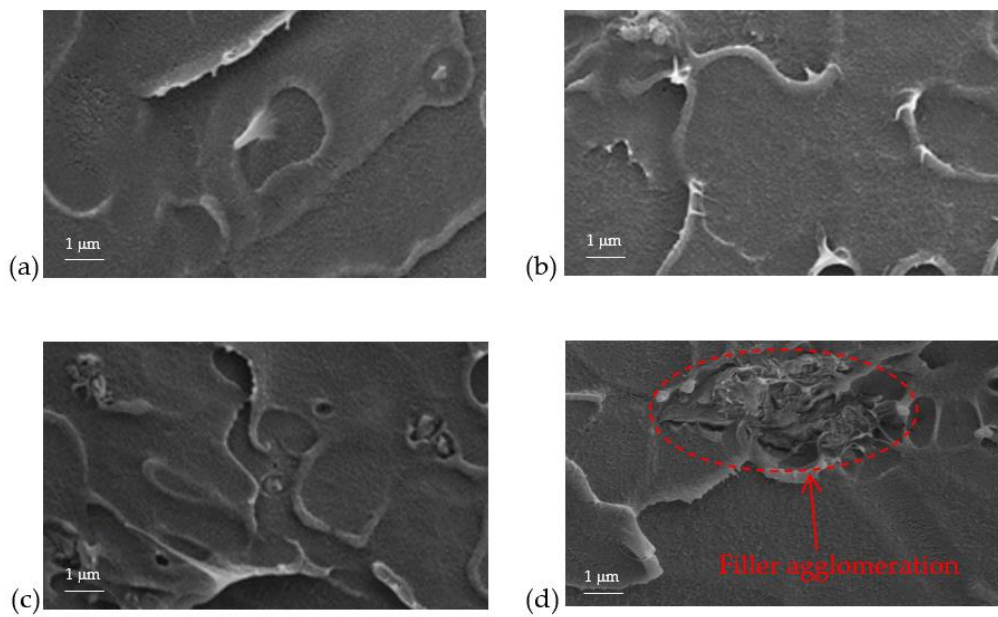


Figure 6. The cross-sectional view of FESEM images of (a) 1% NH₂KIT-6/PSF, (b) 2% NH₂KIT-6/PSF, (c) 3% NH₂KIT-6/PSF, and (d) 4% NH₂KIT-6/PSF.

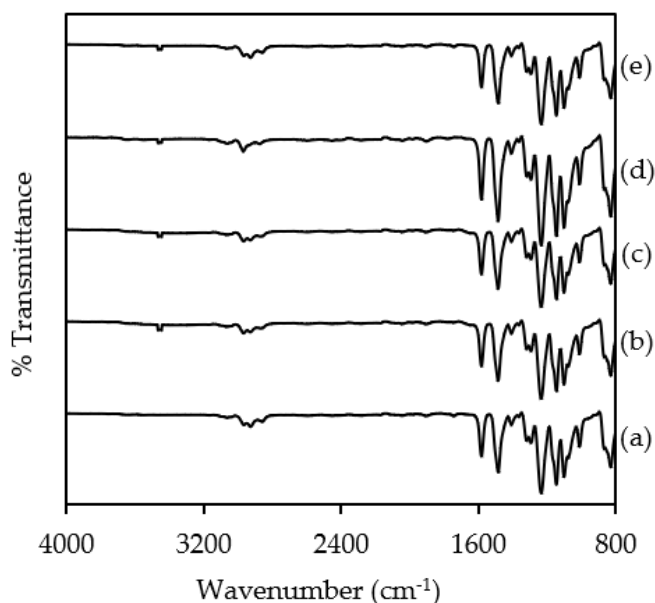


Figure 7. FTIR spectra of (a) PSF, (b) 1% NH₂KIT-6/PSF, (c) 2% NH₂KIT-6/PSF, (d) 3% NH₂KIT-6/PSF, and (e) 4% NH₂KIT-6/PSF.

3.3. Gas Permeation and Separation Studies

Figures 8 and 9 show the CO₂ permeability and CH₄ permeability of the membranes incorporated with different NH₂KIT-6 loadings. The error for the CO₂ permeability and CH₄ permeability was $\pm 5\%$. As observed in Figure 8, the CO₂ permeability increased when NH₂KIT-6 loading in the MMMs was increased. At a pressure difference of 5 bar, an increase of about 47% in ideal CO₂/CH₄ selectivity was achieved by incorporating 2 wt% NH₂KIT-6 into the MMMs. As observed in Figures 8 and 9, the CO₂ permeability and CH₄ permeability decreased when the pressure difference increased from 5 to 7 bar. This is a common behavior of glassy polymers [31,32]. Biondo et al. [33] reported a decrease in CO₂ permeability when the pressure increased for PSF and it was explained that the behavior was typical for a dual-mode model. Figure 10 shows the ideal CO₂/CH₄ selectivity of the membranes incorporated with different NH₂KIT-6 loadings. After the functionalization of KIT-6, the presence of amine groups on NH₂KIT-6 in the MMMs enhanced the affinity of MMMs toward CO₂ and hence increased the ideal CO₂/CH₄ selectivity of the MMMs [14]. However, further increasing the NH₂KIT-6 loading from 2 to 4 wt% caused a drop in the ideal CO₂/CH₄ selectivity, as observed in Figure 10. This might be due to the filler agglomeration in the MMMs, which started to occur at higher NH₂KIT-6 loading. In addition, the gas permeability and ideal CO₂/CH₄ selectivity of the MMMs incorporated with pristine (unfunctionalized) KIT-6 were reported in our earlier work [34]. The MMMs incorporated with NH₂KIT-6 in the current study displayed higher ideal CO₂/CH₄ selectivity compared to MMMs incorporated with the same loadings of pristine KIT-6 in our earlier work [34]. However, the gas permeation and separation performance of the NH₂KIT-6/PSF MMMs in the current study fall below the Robeson upper bound [35]. Hence, future research work is still needed in order to further enhance the gas permeation and separation performance of the NH₂KIT-6/PSF. Table 1 shows the comparison of CO₂ permeability and ideal CO₂/CH₄ selectivity between MMMs from the current study and MMMs incorporated with functionalized silica reported in the literature. The CO₂ permeability obtained in the current study is quite comparable with the CO₂ permeability reported in several other studies. As compared with the research works reported in Table 1, a relatively higher ideal CO₂/CH₄ selectivity was achieved by incorporating 2 wt% NH₂KIT-6 filler into the MMMs in the current study.

Table 1. Comparison of CO₂ permeability and ideal CO₂/CH₄ selectivity between MMMs from current study and MMMs incorporated with functionalized silica reported in the literature.

Polymer/Filler	Amine Group Used for the Filler Functionalization	Filler Loading (wt%)	CO ₂ Permeability (Barrer)	Ideal CO ₂ /CH ₄ Selectivity	Reference
Pebax/MCM-41	Polyethylenimine	5	~87	~23	[14]
PSF/RHS	4-aminophenazone	10	~5.6	~28.1	[1]
PSF/MCM-41	Aminopropyltrimethoxysilane	10	~6.2	~28.0	[13]
PSF/MCM-41	3-aminopropyltriethoxysilane	20	~7.3	~28.1	[11]
PSF/NH ₂ KIT-6	(3-Aminopropyl) triethoxysilane	2	~5.4	~32.4	Current study

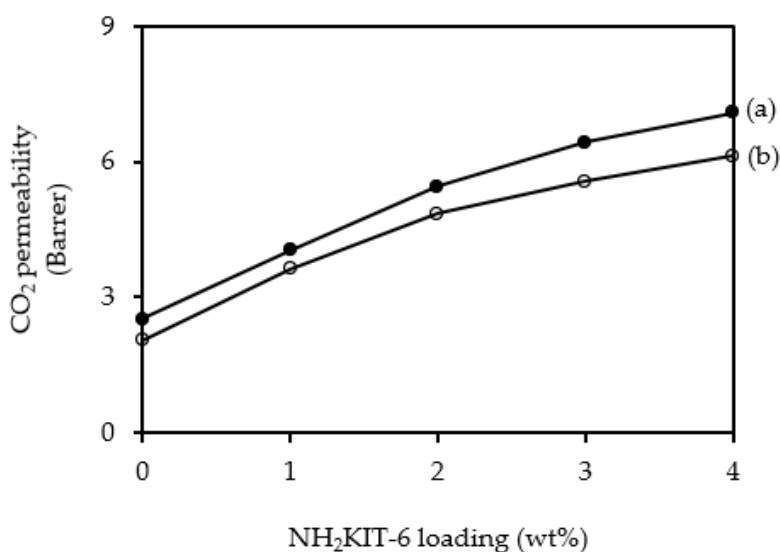


Figure 8. CO₂ gas permeability of the membranes incorporated with different NH₂KIT-6 loadings at pressure differences of (a) 5 bar and (b) 7 bar.

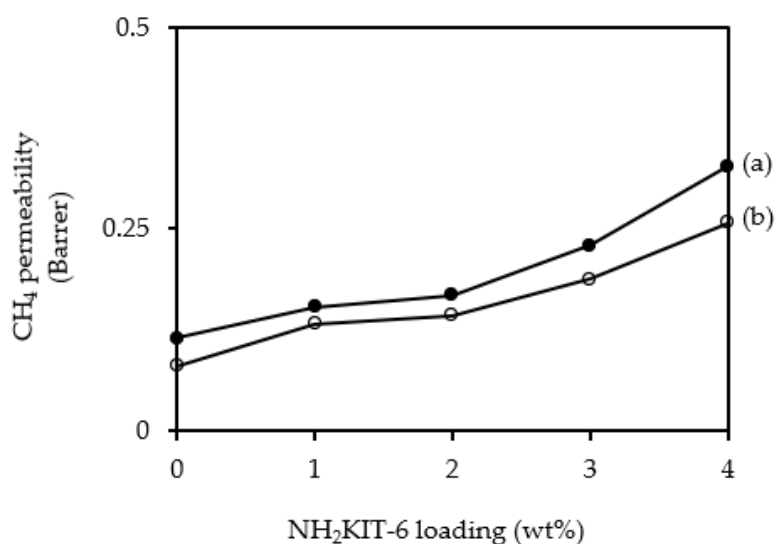


Figure 9. CH₄ gas permeability of the membranes incorporated with different NH₂KIT-6 loadings at pressure differences of (a) 5 bar and (b) 7 bar.

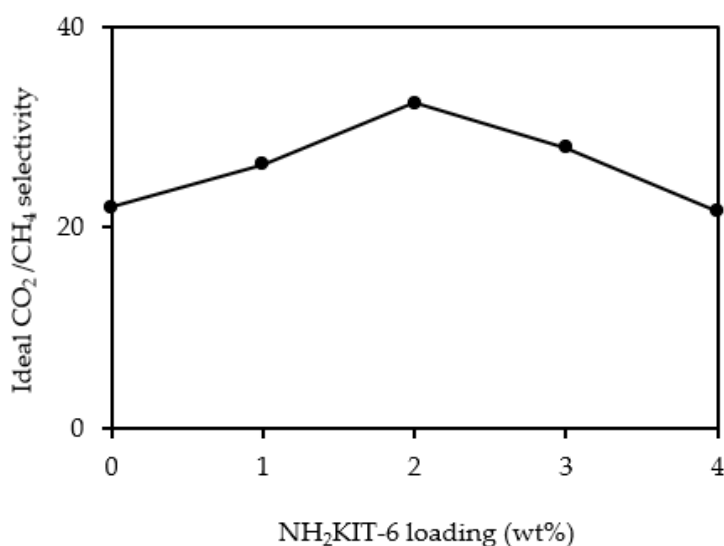


Figure 10. Ideal CO₂/CH₄ selectivity of the membranes incorporated with different NH₂KIT-6 loadings at a pressure difference of 5 bar.

4. Conclusions

In the current study, functionalized KIT-6 (NH₂KIT-6) was incorporated into a PSF matrix to form MMMs. The presence of particles in the MMMs as observed in the FESEM images indicated the successful incorporation of NH₂KIT-6 into the MMMs. The CO₂ permeability and CH₄ permeability decreased when the pressure difference increased from 5 to 7 bar. MMMs with no void in the matrix were successfully fabricated by incorporating up to 2 wt% NH₂KIT-6 into the MMMs. Subsequently, an increase of about 47% in the ideal CO₂/CH₄ selectivity was achieved by incorporating 2 wt% NH₂KIT-6 into the MMMs. However, filler agglomeration started to occur in the MMMs when a higher NH₂KIT-6 loading was incorporated into the MMMs. The ideal CO₂/CH₄ selectivity dropped when the NH₂KIT-6 loading was increased from 2 to 4 wt%.

Author Contributions: Conceptualization, T.L.C. and P.C.O.; methodology, S.H.D. and T.L.C.; investigation, S.H.D.; formal analysis, S.H.D., T.L.C., and P.C.O.; supervision, T.L.C., P.C.O., and A.L.A.; writing—original draft, S.H.D.; writing—review and editing, T.L.C., P.C.O., A.L.A., and C.-D.H. All authors have read and agreed to the published version of the manuscript.

Funding: This research was funded by the Long Term Research Grant Scheme (LRGS, grant number: 304/PJKIMIA/6050296/U124) and the APC was funded by YUTP-Fundamental Research Grant (Cost center: 015LC0-258).

Acknowledgments: This research work was supported by Universiti Teknologi PETRONAS, Institute Contaminant Management UTP, and CO₂ Research Centre (CO2RES). The author would also like to acknowledge the support from YUTP-Fundamental Research Grant (Cost center: 015LC0-258) and Long Term Research Grant Scheme (LRGS) (cost center: 0153AB-L12).

Conflicts of Interest: The authors declare no conflict of interest. The funders had no role in the design of the study; in the collection, analyses, or interpretation of data; in the writing of the manuscript, or in the decision to publish the results.

References

1. Waheed, N.; Mushtaq, A.; Tabassum, S.; Gilani, M.A.; Ilyas, A.; Ashraf, F.; Jamal, Y.; Bilal, M.R.; Khan, A.U.; Khan, L.A. Mixed matrix membranes based on polysulfone and rice husk extracted silica for CO₂ separation. *Sep. Purif. Technol.* **2016**, *170*, 122–129. [[CrossRef](#)]
2. Rezakazemi, M.; Sadrzadeh, M.; Matsuura, T. Thermally stable polymers for advanced high-performance gas separation membranes. *Prog. Energy Combust. Sci.* **2018**, *66*, 1–41. [[CrossRef](#)]

3. Lee, S.; Park, S.C.; Kim, T.Y.; Kang, S.W.; Kang, Y.S. Direct molecular interaction of CO₂ with KTFSI dissolved in Pebax 2533 and their use in facilitated CO₂ transport membranes. *J. Membr. Sci.* **2018**, *548*, 358–362. [[CrossRef](#)]
4. Wang, J.H.; Li, Y.; Zhang, Z.S.; Hao, Z.P. Mesoporous KIT-6 silica–polydimethylsiloxane (PDMS) mixed matrix membranes for gas separation. *J. Mater. Chem. Acad.* **2015**, *3*, 8650–8658. [[CrossRef](#)]
5. Jomekian, A.; Pakizeh, M.; Mansoori, S.A.A.; Poorafshari, M.; Hemmati, M.; Ataee, D.P. Gas transport behavior of novel modified MCM-48/ Polysulfone mixed matrix membrane coated by PDMS. *J. Membr. Sci. Technol.* **2011**, *1*, 1–6.
6. Yavaria, M.; Okamoto, Y.; Lina, H. The role of halogens in polychlorotrifluoroethylene (PCTFE) in membrane gas separations. *J. Membr. Sci.* **2018**, *548*, 380–389. [[CrossRef](#)]
7. Li, S.; Jiang, X.; Sun, H.; He, S.; Zhang, L.; Shao, L. Mesoporous dendritic fibrous nanosilica (DFNS) stimulating mixed matrix membranes towards superior CO₂ capture. *J. Membr. Sci.* **2019**, *586*, 185–191. [[CrossRef](#)]
8. Wang, X.; Ding, X.; Zhao, H.; Fu, J.; Xin, Q.; Zhang, Y. Pebax-based mixed matrix membranes containing hollow polypyrrole nanospheres with mesoporous shells for enhanced gas permeation performance. *J. Membr. Sci.* **2020**, *602*, 117968. [[CrossRef](#)]
9. Li, X.; Yu, S.; Li, K.; Ma, C.; Zhang, J.; Li, H.; Chang, X.; Zhu, L.; Xue, Q. Enhanced gas separation performance of Pebax mixed matrix membranes by incorporating ZIF-8 in situ inserted by multiwalled carbon nanotubes. *Sep. Purif. Technol.* **2020**, *248*, 117080. [[CrossRef](#)]
10. Guo, Z.; Zheng, W.; Yan, X.; Dai, Y.; Ruan, X.; Yang, X.; Li, X.; Zhang, N.; He, G. Ionic liquid tuning nanocage size of MOFs through a two-step adsorption/infiltration strategy for enhanced gas screening of mixed-matrix membranes. *J. Membr. Sci.* **2020**, *605*, 118101. [[CrossRef](#)]
11. Kim, S.; Marand, E. High permeability nano-composite membranes based on mesoporous MCM-41 nanoparticles in a polysulfone matrix. *Microporous Mesoporous Mater.* **2008**, *114*, 129–136. [[CrossRef](#)]
12. Kim, H.J.; Yang, H.C.; Chung, D.Y.; Yang, I.H.; Choi, Y.J.; Moon, J.K. Functionalized Mesoporous Silica Membranes for CO₂ Separation Applications. *J. Chem.* **2015**, *2015*, 1–9.
13. Khan, A.L.; Klaysom, C.; Gahlaut, A.; Vankelecom, I.F.J. Polysulfone acrylate membranes containing functionalized mesoporous MCM-41 for CO₂ separation. *J. Membr. Sci.* **2013**, *436*, 145–153. [[CrossRef](#)]
14. Wu, H.; Li, X.Q.; Li, Y.F.; Wang, S.F.; Guo, R.L.; Jiang, Z.Y.; Wu, C.; Xin, Q.P.; Lu, X. Facilitated transport mixed matrix membranes incorporated with amine functionalized MCM-41 for enhanced gas separation properties. *J. Membr. Sci.* **2014**, *465*, 78–90. [[CrossRef](#)]
15. Mohamad, M.B.; Fong, Y.Y.; Shariff, A. Gas separation of carbon dioxide from methane using polysulfone membrane incorporated with Zeolite-T. *Procedia Eng.* **2016**, *148*, 621–629. [[CrossRef](#)]
16. Aroon, M.A.; Ismail, A.F.; Montazer-Rahmati, M.M.; Matsuura, T. Morphology and permeation properties of polysulfone membranes for gas separation: Effects of non-solvent additives and co-solvent. *Sep. Purif. Technol.* **2010**, *72*, 194–202. [[CrossRef](#)]
17. Bastani, D.; Esmaeili, N.; Asadollahi, M. Polymeric mixed matrix membranes containing zeolites as a filler for gas separation applications: A review. *J. Ind. Eng. Chem.* **2013**, *19*, 375–393. [[CrossRef](#)]
18. Brunetti, A.; Scura, F.; Barbieri, G.; Drioli, E. Membrane technologies for CO₂ separation. *J. Membr. Sci.* **2010**, *359*, 115–125. [[CrossRef](#)]
19. Shahid, S.; Nijmeijer, K. Matrimid®/polysulfone blend mixed matrix membranes containing ZIF-8 nanoparticles for high pressure stability in natural gas separation. *Sep. Purif. Technol.* **2017**, *189*, 90–100. [[CrossRef](#)]
20. Kishor, R.; Ghoshal, A.K. APTES grafted ordered mesoporous silica KIT-6 for CO₂ adsorption. *J. Chem. Eng.* **2015**, *262*, 882–890. [[CrossRef](#)]
21. Kim, W.G.; Lee, J.S.; Bucknall, D.G.; Koros, W.J.; Nair, S. Nanoporous layered silicate AMH-3/cellulose acetate nanocomposite membranes for gas separations. *J. Membr. Sci.* **2013**, *441*, 129–136. [[CrossRef](#)]
22. Ayad, M.M.; Salahuddin, N.A.; El-Nasr, A.A.; Torad, N.L. Amine functionalized mesoporous silica KIT-6 as a controlled release drug delivery carrier. *Microporous Mesoporous Mater.* **2016**, *229*, 166–177. [[CrossRef](#)]
23. Nigar, H. Amine-functionalized mesoporous silica: A Mater. capable of CO₂ adsorption and fast regeneration by microwave heating. *Am. Inst. Chem. Eng.* **2016**, *62*, 547–555. [[CrossRef](#)]

24. Arthanareeswaran, G.; Thanikaivelan, P.; Srinivasn, K.; Mohan, D.; Rajendran, M. Synthesis, characterization and thermal studies on cellulose acetate membranes with additive. *Eur. Polym. J.* **2004**, *40*, 2153–2159. [[CrossRef](#)]
25. Hafizi, H.; Chermahini, A.N.; Saraji, M.; Mohammadnezhad, G. The catalytic conversion of fructose into 5-hydroxymethylfurfural over acid-functionalized KIT-6, an ordered mesoporous silica. *Chem. Eng. J.* **2016**, *294*, 380–388. [[CrossRef](#)]
26. Tzi, E.C.N.; Ching, O.P. Surface modification of AMH-3 for development of mixed matrix membranes. *Procedia Eng.* **2016**, *148*, 86–92. [[CrossRef](#)]
27. Richard, C.; Hing, K.; Schreiber, H.P. Interaction balances and properties of filled polymers. *Polym. Compos.* **1985**, *6*, 201–208. [[CrossRef](#)]
28. Liu, C.S.; Pilania, G.; Wang, C.C.; Ramprasad, R. How critical are the van der Waals interactions in polymer crystals? *J. Phys. Chem.* **2012**, *2012*, 1–19. [[CrossRef](#)]
29. Zornoza, B.; Irusta, S.; Tellez, C.; Coronas, J. Mesoporous silica sphere-polysulfone mixed matrix membranes for gas separation. *Langmuir* **2009**, *25*, 5903–5909. [[CrossRef](#)]
30. Khadary, N.H.; Abdelsalam, M.E. Polymer-silica nanocomposite membranes for CO₂ capturing. *Arab. J. Chem.* **2017**, *2017*, 1–10. [[CrossRef](#)]
31. Lasseguette, E.; Malpass-Evans, R.; Carta, M.; McKeown, N.B.; Ferrari, M.-C. Temperature and pressure dependence of gas permeation in a microporous Troger's base polymer. *Membranes* **2018**, *8*, 132. [[CrossRef](#)] [[PubMed](#)]
32. Li, P.; Chung, T.S.; Paul, D.R. Gas sorption and permeation in PIM-1. *J. Membr. Sci.* **2013**, *432*, 50–57. [[CrossRef](#)]
33. Biondo, L.D.; Duarte, J.; Zeni, M.; Godinho, M.A. Dual-mode interpretation of CO₂/CH₄ permeability in polysulfone membranes at low pressures. *Anais Acad. Bras. Cienc.* **2018**, *90*, 1855–1864. [[CrossRef](#)] [[PubMed](#)]
34. Ding, S.H.; Ng, T.Y.S.; Chew, T.L.; Oh, P.C.; Ahmad, A.L.; Ho, C.-D. Evaluation of the properties, gas permeability and selectivity of mixed matrix membrane based on polysulfone polymer matrix incorporated with KIT-6 silica. *Polymers* **2019**, *11*, 1732. [[CrossRef](#)]
35. Robeson, L.M. The upper bound revisited. *J. Membr. Sci.* **2008**, *320*, 390–400. [[CrossRef](#)]



© 2020 by the authors. Licensee MDPI, Basel, Switzerland. This article is an open access article distributed under the terms and conditions of the Creative Commons Attribution (CC BY) license (<http://creativecommons.org/licenses/by/4.0/>).